Journal of Hydrology (2008) **348**, 279–291

available at www.sciencedirect.com

ScienceDirect

journal homepage: www.elsevier.com/locate/jhydrol

Re-conceptualizing the soil and water assessment tool (SWAT) model to predict runoff from variable source areas

Zachary M. Easton [a,*], Daniel R. Fuka [a], M. Todd Walter [a], Dillon M. Cowan [b], Elliot M. Schneiderman [c], Tammo S. Steenhuis [a]

[a] *Department of Biological and Environmental Engineering, Cornell University, Ithaca, NY 14853, USA*
[b] *School of Civil and Environmental Engineering, Cornell University, Ithaca, NY 14853, USA*
[c] *New York City Department of Environmental Protection, 71 Smith Avenue, Kingston, NY 12401, USA*

Received 6 May 2007; received in revised form 29 September 2007; accepted 1 October 2007

KEYWORDS
Water quality;
Non-point source pollution;
Saturation excess;
Distributed model;
Curve-number (CN);
Variable source area (VSA)

Summary Many water quality models use some form of the Natural Resources Conservation Services (formerly Soil Conservation Service) curve number (CN) equation to predict storm runoff in ways that implicitly assume an infiltration-excess response to rainfall. Because of this, these models may fail to predict variable source areas (VSAs) correctly, i.e. where runoff is typically generated in rural, humid regions. In this study, the Soil and Water Assessment Tool (SWAT) model was re-conceptualized to distribute overland flow in ways consistent with VSA hydrology by modifying how the CN and available water content were defined; the new modeling approach is called SWAT-VSA. Both SWAT and SWAT-VSA were applied to a sub-watershed in the Cannonsville basin in upstate New York to compare model predictions of integrated and distributed responses, including surface runoff, shallowly perched water table depth, and stream phosphorus loads against direct measures. Event runoff was predicted similarly well for SWAT-VSA and SWAT. However, the distribution of shallowly perched water table depth was predicted better by SWAT-VSA and it is this shallow groundwater that governs VSAs. Event based dissolved phosphorus export from the watershed was also predicted better by SWAT-VSA, presumably because the distribution of runoff source areas was better predicted particularly from areas where manure was applied. This has important consequences for using models to evaluate and guide watershed management because correctly predicting where runoff is generated is critical to locating best management practices to control non-point source pollution.

* Corresponding author. Tel.: +1 607 255 2463.
E-mail address: zme2@cornell.edu (Z.M. Easton).

0022-1694/$ - see front matter
doi:10.1016/j.jhydrol.2007.10.008

Introduction

Water quality modeling is an important tool used by researchers, planners, and government agencies to optimize management practices to improve water quality. Many of these water quality models use some form of the Natural Resources Conservation Services (formerly Soil Conservation Service) curve number (CN) equation to predict storm runoff from watersheds. The way the CN is applied in these models implicitly assumes an infiltration-excess (or Hortonian, i.e., Horton, 1933) response to rainfall (Walter and Shaw, 2005). However, in humid, well-vegetated regions, especially those with permeable soils underlain by a shallow restricting layer, storm runoff is usually generated by saturation-excess processes on variable source areas (VSAs) (Dunne and Black, 1970; Dunne and Leopold, 1978; Beven, 2001; Srinivasan et al., 2002; Needelman et al., 2004). Thus, many of the most commonly used water quality models do not correctly capture the spatial distribution of runoff source areas and, by association, pollutant source areas (Qui et al., 2007). Examples of models using a CN-type approach include the Generalized Watershed Loading Function (GWLF) model (Haith and Shoemaker, 1987), the Soil Water Assessment Tool (SWAT) model (Arnold et al., 1998), the Storm Water Management Model (SWMM) (Krysanova et al., 1998), the Erosion Productivity Impact Calculator (EPIC) model (Williams et al., 1984), and the Long-Term Hydrologic Impact Assessment (L-THIA) model (Bhaduri et al., 2000). Although these models have routinely been calibrated to correctly predict stream discharge and sometimes stream water quality at the watershed outlet this does not mean that distributed hydrological processes were correctly captured (Srinivasan et al., 2005). Indeed, lumped models, which implicitly ignore how intra-watershed processes are distributed, can predict integrated watershed responses like stream flow as well as models that simulate a fully distributed suite of intra-watershed processes (Franchini and Pacciani, 1991; Johnson et al., 2003).

Watershed managers tasked with implementing strategies for controlling non-point source (NPS) pollution need water quality models that can correctly identify the locations where runoff is generated in order to effectively place best management practices (BMPs). Although, as discussed earlier, most current water quality models do not have this capacity, Lyon et al. (2004), building on Steenhuis et al. (1995), showed how CN models can be used to predict the distribution of VSAs. Schneiderman et al. (in press) were the first to use this body of work to modify an existing water quality model, namely GWLF (Haith and Shoemaker, 1987), so that it explicitly simulated saturation excess runoff from VSAs.

It is challenging to modify more complex models like SWAT or EPIC because many of their sub-models, especially those simulating various biogeochemical processes, have been developed around the assumption that a watershed can be characterized by an assemblage of non-interacting landscape-units delineated by land use and soil type. While this is perhaps a reasonable assumption when considering deep soil profiles without restricting layers or shallow water tables and, hence, areas where surface runoff is primarily produced when the rainfall intensity exceed the infiltration capacity of the soil (i.e., Hortonian or infiltration-excess runoff), it may not prove accurate in VSA dominated areas. In many areas, VSAs are formed when shallow ground water flowing within the soil from upslope areas of the watershed accumulates and saturates lower parts of the watershed. These VSAs become ''active'' when groundwater flow exceeds storage or when precipitation falls on the saturated area, causing saturation excess runoff. This concept necessitates recognizing interactions throughout the landscape. Thus, the challenge of incorporating VSA hydrology into models employing CN-type functionality is to find ways of capturing the spatial arrangement of saturation excess runoff source areas while also retaining the soil and land use information necessary to various nutrient and biogeochemical subroutines.

This study specifically focused on SWAT, one of the most commonly used and well supported water quality modeling systems available. The strengths of SWAT are its use of readily available input data and its process based nutrient biogeochemistry sub-models (Santhi et al., 2001; van Griensven and Bauwens, 2003; Borah and Bera, 2004; Ramanarayanan et al., 2005). Storm runoff is predicted with the CN equation, which we have already noted can be used in a VSA context. SWAT divides sub-basins into hydrological response units (HRUs) but currently does not allow water flow among HRUs and, therefore, cannot simulate the formation of VSAs. In this investigation we propose using a topographic wetness index to redefine HRUs so that spatial runoff patterns would follow those observed in VSA dominated landscapes. Indeed, Lyon et al. (2004) found that topographic indices described the evolution of a shallow water table in the Catskill Mountain of New York and that this shallow water table was the primary control on VSA formation. One of the earliest uses of topographic wetness indices to simulate VSA hydrology was TOPMODEL (Beven and Kirkby, 1979) and the topographic index concept has since been applied outside of TOPMODEL and found to effectively predict VSAs for many watersheds dominated by saturation-excess runoff (Western et al., 1999; Lyon et al., 2004; Agnew et al., 2006; Schneiderman et al., in press). This re-conceptualization of SWAT allows users to model and predict saturation excess runoff from VSAs without modifying the code base, and thus provides a simple means of capturing spatially variant saturation excess runoff processes from the landscape. The re-conceptualized version of SWAT, referred to as SWAT-VSA, is tested using integrated watershed responses at a watershed outlet and spatially-distributed data from within a watershed. We also compared SWAT-VSA predictions to those made by a standard implementation of SWAT.

Summarized SWAT description

The SWAT model is a river basin or watershed scale model created to run with readily available input data so that general initialization of the modeling system does not require overly complex data gathering or calibration. SWAT was originally intended to model long-term runoff and nutrient losses from rural watersheds, particularly those dominated by agriculture (Arnold et al., 1998). SWAT requires soils data, land use/management information, and elevation data to drive flows and direct sub-basin routing. While these data may be spatially explicit, SWAT lumps the parameters into hydrologic response units (HRU), effectively ignoring the underlying spatial distribution. Traditionally, HRUs are defined by the coincidence of soil type (Hydrologic Soil Group, USDA, 1972) and land use. Simulations require meteorological input data including precipitation, temperature, and solar radiation. In the present study, model input data and parameters were initially parsed using the AVSWATX interface (Di Luzio et al., 2000). The interface assimilated the soil input map, digital elevation model, and land use coverage.

CN equation applied to VSA theory

SWAT-VSA capitalizes on the re-conceptualization of the CN equation to capture VSA storm hydrology (Steenhuis et al., 1995; Lyon et al., 2004; Schneiderman et al., in press), which we will briefly summarize the background of here. The CN equation was originally developed by Mockus (Rallison, 1980) and estimates total watershed runoff depth Q (mm) (both overland flow and rapid subsurface flow) for a storm (USDA-SCS, 1972):

$$Q = \frac{P_e^2}{P_e + S_e} \tag{1}$$

where P_e (mm) is the depth of effective rainfall after runoff begins, i.e. rainfall minus initial abstraction, I_a (rainfall retained in the watershed when runoff begins) and S_e (mm) is the depth of effective available storage in the watershed, or the available volume of retention in the watershed when runoff begins. I_a is estimated as an empirically-derived fraction of available watershed storage (USDA-SCS, 1972).

Steenhuis et al. (1995) showed that Eq. (1) could be interpreted in terms of a saturation-excess process. Assuming that all rain falling on unsaturated soil infiltrates and that all rain falling on areas that are saturated becomes runoff, then the rate of runoff generation will be proportional to the fraction of the watershed that is effectively saturated, A_f, which can then be written as:

$$A_f = \frac{\Delta Q}{\Delta P_e} \tag{2}$$

where ΔQ is incremental saturation-excess runoff or, more precisely, the equivalent depth of excess rainfall generated during a time period over the whole watershed area, and ΔP_e is the incremental depth of precipitation during the same period. Thus, by differentiating Eq. (1) with respect to P_e, the fractional contributing area for a storm can be written as (Steenhuis et al., 1995):

$$A_f = 1 - \frac{S^2}{(P_e + S_e)^2} \tag{3}$$

According to Eq. (3), runoff only occurs from areas that have a local effective available storage, σ_e (mm), less than P_e. Therefore, by substituting σ_e for P_e in Eq. (3) we have a relationship for the fraction of the watershed area, A_s, that has a local effective soil water storage less than or equal to σ_e for a given overall watershed storage of S_e (Schneiderman et al., in press):

$$A_s = 1 - \frac{S_e^2}{(\sigma_e + S_e)^2} \tag{4}$$

Note that that both S_e and I_a are watershed properties while $\sigma_e$is defined at the local level. Solving for σ_e gives the maximum effective local soil moisture storage within any particular fraction, A_s, of the watershed area (Schneiderman et al., in press):

$$\sigma_e = S_e\left(\sqrt{\frac{1}{(1 - A_s)}} - 1\right) \tag{5}$$

For a given storm event with precipitation P, the fraction of the watershed that saturates first ($A_s = 0$) has local storage $\sigma_e = 0$, and runoff from this fraction will be $P - I_a$. Successively drier fractions retain more precipitation and produce less runoff according to the moisture – area relationship of Eq. (5). The driest fraction of the watershed that saturates during a storm defines the total contributing area (A_f). As average effective soil moisture storage (S_e) changes through the year, the moisture-area relationship will shift accordingly (Eq. (5)); S_e is constant once runoff begins.

According to Schneiderman et al. (in press), runoff for an area, q_i (mm), can be expressed as:

$$q_i = P_e - \sigma_e \quad \text{for } P_e > \sigma_e, \tag{6}$$

For $P_e \leqslant \sigma_e$, the unsaturated portion of the watershed, $q_i = 0$. To avoid changing any SWAT code, we propose approximating Eq. (6) with the CN equation (Fig. 1):

$$q_i = \frac{P_e^2}{P_e + \sigma_e} \tag{7}$$

This approximation gives the same result when $P \to \infty$ satisfying the boundary condition. However, runoff starts earlier as shown in (Fig. 1). Thus, unlike Eqs. (6) and (7) predicts some flow before the local soil deficit is filled, which may be interpreted as early, rapid subsurface flow or as an uneven distribution of storages (σ_e) within the runoff producing area.

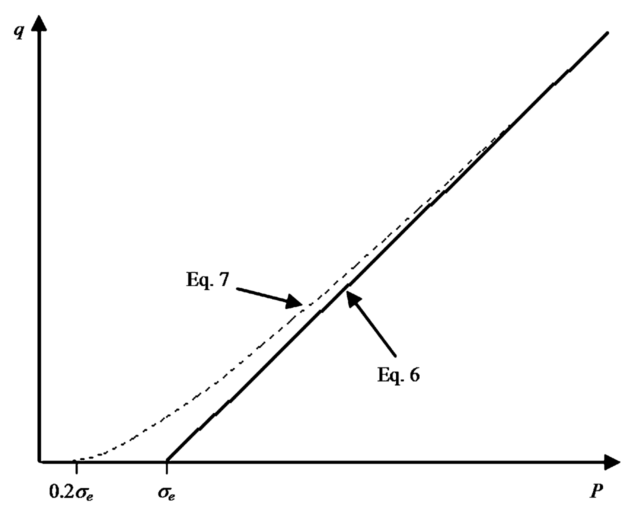

Figure 1 Comparison between the saturation excess version of the CN equation, Eq. (6) ($P_e = P - 0.2\sigma_e$) (Schneiderman et al., in press), and the SWAT-VSA approximation, Eq. (7).

Implementation for variable source areas (VSAs)

The most significant part of our re-conceptualization of SWAT lies in re-defining HRUs. Following Schneiderman et al. (in press), we use a topographic wetness index in combination with land use to define the HRUs. Specifically, we use a soil topographic index (STI) (e.g., Beven and Kirkby, 1979):

$$\mathrm{STI} = \ln\left(\frac{a}{T\tan\beta}\right) \tag{8}$$

where a is the upslope contributing area for the cell per unit of contour line (m), $\tan\beta$ is the topographic slope of the cell, and T is the transmissivity (soil depth $\times$ saturated soil hydraulic conductivity) of the uppermost layer of soil ($m^2\,d^{-1}$) (Lyon et al., 2004). The local storage deficit of each wetness class ($\sigma_{e,i}$) is determined by integrating Eq. (5) over the fraction of the watershed represented by that wetness index class (Schneiderman et al., in press):

$$\sigma_{e,i} = \frac{2S_e\left(\sqrt{1-A_{s,i}} - \sqrt{1-A_{s,i+1}}\right)}{(A_{s,i+1} - A_{s,i})} - S_e \tag{9}$$

where the fractional area represented by each index class is bounded on one side by the fraction of the watershed that is wetter, $A_{s,i}$, i.e., the part of the watershed that has lower local moisture storage, and on the other side by the fraction of the watershed that is dryer, $A_{s,i+1}$, i.e., has greater local moisture storage. Index classes are numbered from 1, the driest and least prone to saturate, to n, the most frequently saturated.

In the standard version of SWAT land use and soil type define the area of each HRU. In SWAT-VSA the area of each HRU is defined by the coincidence of land use and wetness index class determined from the STI (Eq. (8)); Fig. 2 shows how HRUs are delineated in the SWAT-VSA framework. The additional information necessary for SWAT's nutrient and biogeochemical subroutines, specifically, topology (e.g. slope position and length, etc) and various soil physical and chemical properties, are averaged within each wetness index class. We do not anticipate serious problems due to taking average soil properties within an index class because there is evidence that soil variability roughly correlates with topographic features, probably because soil genesis is to a great extent driven by hydrology and topology (Page et al., 2005; Sharma et al., 2006; Thompson et al., 2006).

In SWAT, runoff is calculated for each soil/land-use defined HRU using Eq. (1). In SWAT-VSA, the runoff for each wetness-index-class/land-use defined HRU is calculated with Eq. (7), which is approximately equivalent to Eq. (1) for large events. The difference is that in SWAT-VSA, the effective storage is associated with each HRU's wetness index (Eq. (9)) and in SWAT the effective storage is based on land use and soil infiltration capacity. Note that in SWAT-VSA, runoff depth within a wetness index class will be the same irrespective of land use while nutrient dynamics will

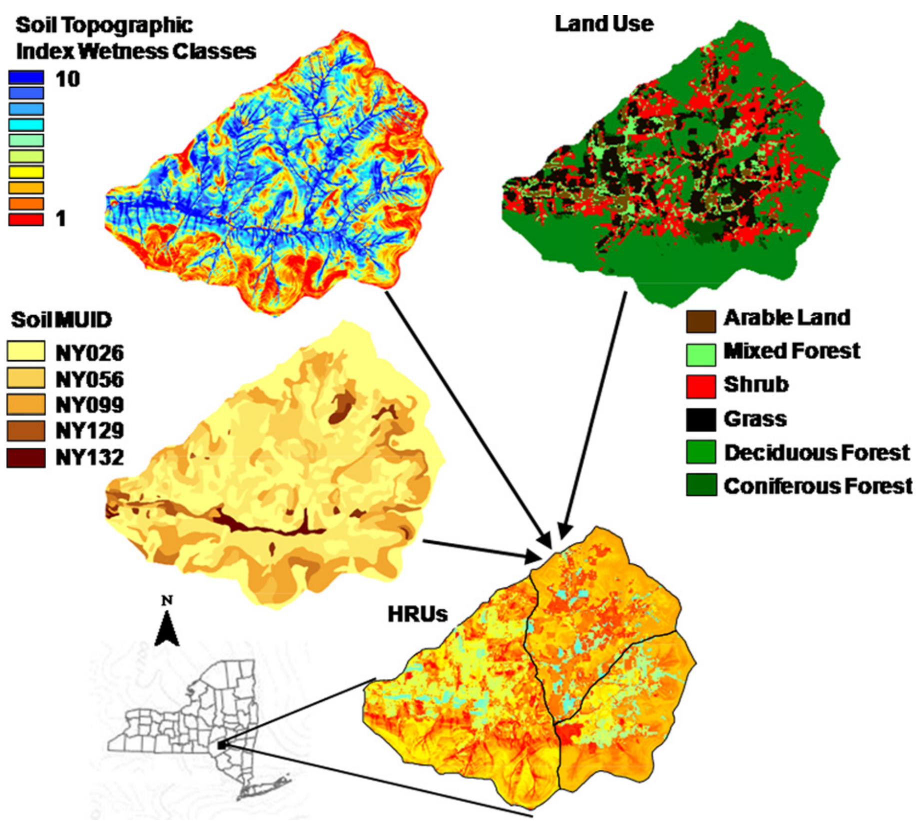

Figure 2 Conceptual framework for implementation of saturation excess runoff from variable source areas into SWAT. Pertinent SSURGO soil information were extracted with an aerially weighted soil topographic index (STI), and included in the index input table by wetness class. Then the STI and land use rasters were intersected to form hydrologic response units (HRU).

vary with land uses and, thus, can differ within index classes. Nutrient loads from each wetness-index-class/land-use HRU are tracked separately in SWAT-VSA, but are otherwise processed similarly to SWAT. For the entire watershed, runoff depth is the aerially-weighted sum of local runoff depths, q_i, for all HRUs.

Although topographic wetness indices capture the spatial patterns of VSAs, the SWAT code does not allow water flow among HRUs. Thus, to compensate for this we propose adjusting the available water content (AWC) of the soil profile so that higher wetness index classes retain water longer, and the lower classes dry quicker. In VSA theory runoff production is related to saturation dynamics, accordingly there needs to be higher water contents in high runoff producing areas, thus we relate local soil water storage, $\sigma_{e,i}$, to AWC with the following relationship:

$$\mathrm{AWC} = \left[\left(1 - \frac{\rho_b}{2.65} - 0.05\right) - \left(\frac{0.4(\mathrm{clay})\rho_b}{100}\right)\right] \times \left(\frac{254}{\sigma_{e,i} + 24.5} \times 0.01\right) \tag{10}$$

where ρ_b is the soil bulk density (g cm^{-3}) and clay is the soil clay content (cm^3 cm^{-3}). Eq. (10) makes conceptual sense in the SWAT-VSA framework because $\sigma_{e,i}$ is directly related to the saturated area by Eq. (4). Notice that the form of last term of Eq. (10) is the same as the relationship between S_e and the CN. Using this relationship the soil moisture in runoff producing areas is forced to a higher level. This calculation is derived and adapted directly from SWAT's own soil water calculations, its soil physics routine (AWC = field capacity − wilting point).

HRUs dominated by impervious surfaces are simulated identically and with the same infiltration-excess approach as used in SWAT.

Watershed description and model applications

We applied both SWAT and SWAT-VSA in the test watershed and compared model predictions to measurements of stream flow and dissolved phosphorus in the stream (data collected by USGS, via M. McHale, personal comm.) and distributed measures of shallow water table depth perched on the shallow bedrock and fragipan restricting layers (Lyon et al., 2006a,b). The USGS sampling protocol at the outlet of the watershed includes both event-based and biweekly (generally baseflow) samples, therefore we compare event based model predictions with event based runoff estimates obtained from baseflow-separation of daily stream hydrograph data (Arnold and Allen, 1999).

Watershed description

The test watershed is a 37 km^2 rural watershed located in the Catskill Mountains of New York State (Fig. 2). The region is typified by steep to moderate hillslopes of glacial origins with shallow permeable soils, underlain by a restrictive layer. The climate is humid with an average annual temperature of 8 °C and average annual precipitation of 1123 mm. Elevation in the watershed ranges from 493 to 989 m above mean sea level with slopes as steep as 43°. Soils are mainly silt loam or silty clay loam with soil hydrologic group C ratings (USDA-NRCS, 2000) (Fig. 2). Soil depth ranges from <50 cm to >1 m and is underlain by a fragipan restricting layer (e.g. coarse-loamy, mixed, active, mesic, to frigid Typic Fragiudepts, Lytic or Typic Dystrudepts common to glacial tills) (Schneiderman et al., 2002). The lowland portion of the watershed is predominantly agricultural, consisting of pasture and arable land (20%), shrub land (18%), and the upper slopes are forested (60%) (Fig. 2). Water and wetland comprise 2%, and impervious surfaces occupy <1% of the watershed and thus both were excluded from consideration in the model. Several studies in this and nearby watersheds have shown that variable source areas control overland flow generation (Frankenberger et al., 1999; Mehta et al., 2004; Lyon et al., 2006a,b; Schneiderman et al., in press) and that infiltration-excess runoff is rare (Walter et al., 2003).

Input data

Spatial Data: Required landscape data includes tabular and spatial soil data, tabular and spatial land use information, and elevation data. All soils data were taken from the SSURGO soil data base (USDA-NRCS, 2000) (Fig. 3); arithmetic means were used for all soils properties for which SSURGO contained a range of values. For SWAT-VSA, we substituted the STI for the soils map to create the HRUs. However, since SWAT requires many soil properties for both the hydrologic and biogeochemical sub-routines we areally weighted the soils map with the STI using GRASS (US Army CERL, 1997) and extracted the associated soils properties from the SSURGO database. These values were then integrated into look up tables and linked to the map in the AVSWATX interface. For SWAT-VSA, we lumped the watershed's STI into 10 equal area intervals ranging from 1 to 10, with index class 1 covering the 10% of the watershed area with the lowest STI (i.e. lowest propensity to saturate) and index class 10 containing the 10% of the watershed with the highest STI (i.e. highest propensity to saturate) (Fig. 2). These wetness index classes were intersected with the land use to create 160 HRUs in three sub-basins (Fig. 2). Sub-basins were defined in the AVSWATX interface by setting a minimum area threshold of 10 km^2 so that each sub-basin compromises an approximately equal area of the watershed (Fig. 2). A digital elevation model (DEM) of the basin was obtained from the New York City Department of Environmental Protection (NYCDEP) with 10 m × 10 m horizontal and 0.1 m vertical resolutions. Land use was remotely sensed by medium resolution satellite data (Landsat 7 ETM+) (de Alwis, 2007) (Fig. 2).

Required Meteorological Data: Daily precipitation data were collected from the four nearest weather stations, specifically, Stamford, Pratsville, Arkville, and Delhi, NY (Northeast Regional Climate Center, NRCC). All weather stations were located outside of the test watershed. The input precipitation for the watershed was determined using an inverse distance squared weighting procedure (distance to watershed centroid) to create one time series. Daily minimum and maximum temperature data were collected at the NRCC station in Stamford, NY, the closest station to the watershed. Daily solar radiation and wind speed data were obtained from the NRCC station in Binghamton, NY. Daily potential evapotranspiration rates were calculated in

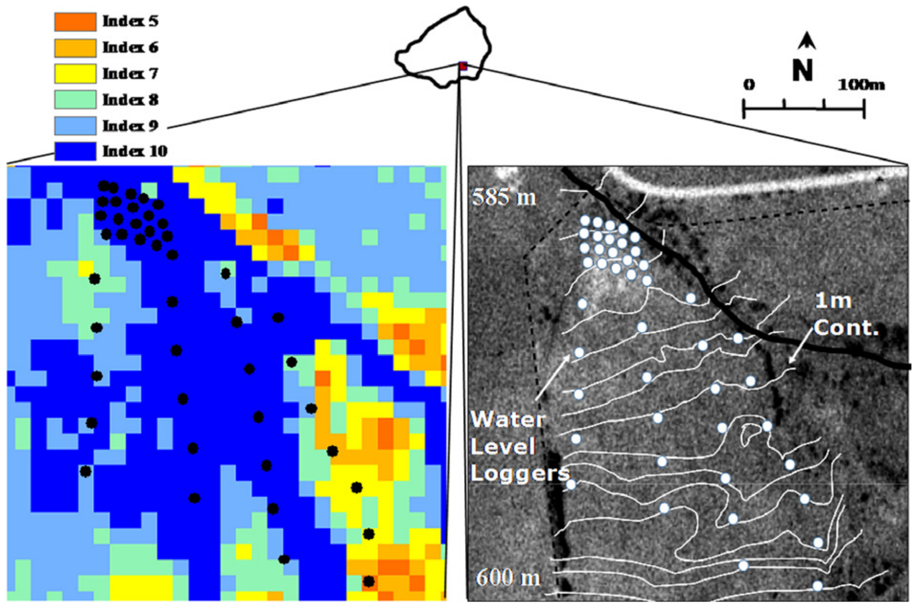

Figure 3 Location of capacitance probes, and elevation gradient in the watershed (right) (from Lyon et al., 2006a). Map on left show the respective index classes spanned by the probes.

the SWAT model using the Penmen–Monteith method. Meteorological stations were geo-referenced (latitude, longitude, and elevation) and the variables adjusted in SWAT using lapse rates in the watershed.

Calibration

A two-step procedure was used to calibrate the CN_{II} values for SWAT-VSA's wetness index classes based on 1998–2001 data. A basin wide storage (S_e) of 16 cm (Lyon et al., 2004) was used to distribute the $\sigma_{e,i}$ values in the basin according to the wetness index (Eq. (9)), which results in a basin-wide average $CN_{II} = 73$ per the method outlined in the model development section (i.e., VSA CN_{II} method, Table 1). This first step established the relative distribution of $\sigma_{e,i}$. Because the CN equation is non-linear, the flow predicted using a lumped S_e will not necessarily be the same as that predicted as the sum of multiple contributing areas, even if the average storage in both cases is the same. Therefore, we re-ran the calibration uniformly adjusting all the CN_{II} (by CN-units of 0.25) to minimize the RMSE between predicted and measured runoff. The optimized average CN_{II}, over all wetness index classes, was 70, which was similar to that found in an earlier study using GWLF for the same cal-

Table 1 Parameters adjusted for SWAT-VSA and SWAT

SWAT-VSA				SWAT		
Wetness index	STI[a]	CN_{II}-VSA[b]	AWC (cm^3 H_2O cm^{-3}) soil	Soil hydrologic group	Land use	CN_{II}[b]
1	5.4	22.97	0.09	C	Shrub	67.21
2	7.6	49.50	0.19	C	Pasture	72.05
3	8.2	61.11	0.25	C	Deciduous forest	70.30
4	8.6	69.56	0.29	C	Evergreen forest	64.52
5	9.1	76.30	0.33	C	Mixed forest	66.29
6	9.6	81.94	0.36	C	Row crop	77.42
7	10.0	86.81	0.38			
8	10.5	91.09	0.41			
9	11.3	94.91	0.44			
10	17.2	98.37	0.45			
Average	9.8	VSA 73, Calibrated 70	0.319			70

Soil topographic index values (STI) for each class, curve number II (CN_{II}) values calculated with the VSA methodology, available water content (AWC), for the index classes used in the SWAT-VSA model CN_{II} used for the standard SWAT model for each land use, and soil hydrologic group (all other parameters were left as SWAT defaults derived by the AVSWATX ArcView Interface).
[a] Average soil topographic index for each wetness index class.
[b] The average CN_{II} values were calibrated from the observed runoff/rainfall relationship at the watershed outlet.

ibration period, CN_{II} = 70.1 (NYCDEP, 2004). The differential between the CN_{II} value of 73, determined using the VSA methodology described above, and the CN_{II} value of 70, determined using the minimization method, is due to the different runoff calculations used (i.e., Eq. (6) vs. Eq. (7)). To insure good calibration, we also made sure that our calibrated result maximized the coefficient of determination (r^2) and the Nash—Suttcliffe efficiency (E) (Nash and Sutcliffe, 1970). Table 1 summarizes the calibrated CN_{II} values for each wetness index class.

Accordingly, to determine the basin average CN_{II} for SWAT we used the same S_e of 16 cm from Lyon et al. (2004) and distributed the CN_{II} values based on tabulated ranges such that the aerially weighted average CN_{II} value was 70. The final CN_{II} value for each HRU was calibrated using the same approach as for SWAT-VSA, i.e., adjusting all the CN_{II} values uniformly to minimize RMSE between predicted and observed runoff (1998—2001) and maximize r^2 and E. The calibrated average-over-all-HRUs CN_{II} = 70, was identical to the CN_{II} for SWAT-VSA. Table 1 summarizes the calibrated CN_{II} values for each combination for soil and land use. Both SWAT-VSA and SWAT were run on daily time steps.

Simulated phosphorus applications

We simulated P applications from fertilizer and manure in the watershed using the nutrient management plan (NMP) obtained from the Delaware County Watershed Agricultural Council for the largest farm in the watershed, which accounted for approximately 50% of the land where P was applied. We followed the rotational and application timing recorded in the NMP, and assumed these applications were representative for the remaining agricultural land in the watershed. Phosphorus application rates were, on average, 90—120 kg ha^{-1} yr^{-1} on agricultural land. Soil test P values from the NMP were used to initialize the labile P in the first soil layer where levels were high (i.e., row crop and pasture land uses). The model was allowed to equilibrate by starting the simulation 2 years before the observed data record began using measured weather data. Default values were used for all P-simulation parameters within SWAT and not adjusted when implementing the NMP.

Validation

We validated SWAT-VSA and SWAT (2002—2004) by comparing both integrated (event runoff and event stream P export) and distributed (distributed water table) predictions to direct measurements. While the model was run on a daily time step, integrated validation was performed on an event basis. For each constituent, model performance was evaluated with four methods: qualitatively using time series plots and quantitatively using the coefficient of determination (r^2), the root mean square error (RMSE), and the Nash—Suttcliffe coefficient (E). To test SWAT and SWAT-VSA's abilities to predict distributed hydrology correctly, we used measurements by Lyon et al. (2006a) of water table height above the restricting layer for a section of the watershed. Briefly, 44 capacitance probes, installed to depths of ~50 cm, recorded the water table height in 15 min intervals from April 2004 to September 2004 (Fig. 3). The field site encompassed five wetness index classes (Fig. 3) and three land use types, pasture, shrub, and mixed forest. To compare the measured and SWAT-VSA water table heights the capacitance probe data were averaged across index classes; there were between two and 32 capacitance probes per index. To compare measured water table heights with SWAT water table heights we averaged across land use; there were four to 32 measurements per land use. SWAT (and SWAT-VSA) reports soil water in mm of water integrated over the soil profile (i.e. cumulative water depth for all soil layers). Thus, we converted the model predicted mm of soil water to and equivalent depth by dividing by the SSURGO reported porosity and assumed the SSURGO reported depth to the restricting layer was accurate. According to the SSURGO database, the depth to the local restricting layer at the measurement site is 1.2—1.4 m.

Results and discussion

Stream flow

SWAT and SWAT-VSA simulated runoff did not differ significantly (p-value < 0.05 paired t-test) as would be expected using the same watershed CN_{II} values (Fig. 4a and b, respectively). Predicted and observed event runoff for both models resulted in Nash-Suttcliffe efficiency greater than 0.7 for both calibration and validation periods (Fig. 4). No systematic bias was evident in the results, with predicted vs. observed data evenly scattered around the 1:1 line (Fig. 4 insets). The largest deviation for both models was for an April 2001 snowmelt event, which both models over predicted by approximately 15%. Fig. 4a and b show that that distributing the S_e differently had little impact on the integrated runoff response. The adjustment of the AWC by index was the cause of the minor deviations between SWAT-VSA and SWAT runoff in Fig. 4a and b.

The major difference is in how the runoff is distributed. For example, Fig. 5 shows the distribution of runoff generation for a November 2003 event. As anticipated, the distribution of predicted runoff generation for SWAT-VSA reflects the imposed topographical controls, with higher runoff associated with HRUs with higher wetness index classes, i.e. areas closer to the stream (Fig. 5a). SWAT's distribution of runoff generation reflects the underlying soils and land use controls that the model assumes. Interestingly, because the farm land in this watershed is located in near stream areas and this land is associated with relatively high infiltration-excess runoff (higher CN_{II} value), SWAT actually predicts its highest runoff from locations similar to SWAT-VSA (Fig. 5a and b). However, SWAT-VSA predicts large portions of the watershed as producing little or no runoff, whereas SWAT predicts runoff from virtually every place in the watershed (Fig. 5b). To illustrate the differences in how SWAT-VSA and SWAT distribute runoff we plotted the cumulative runoff from the different HRUs with a pasture land use (Fig. 6a and b). By definition, SWAT-VSA HRUs with the same wetness index class had the same runoff, but among wetness indices cumulative runoff over the simulation period varied from near zero to >3000 mm (Fig. 6a). There were only three SWAT HRUs

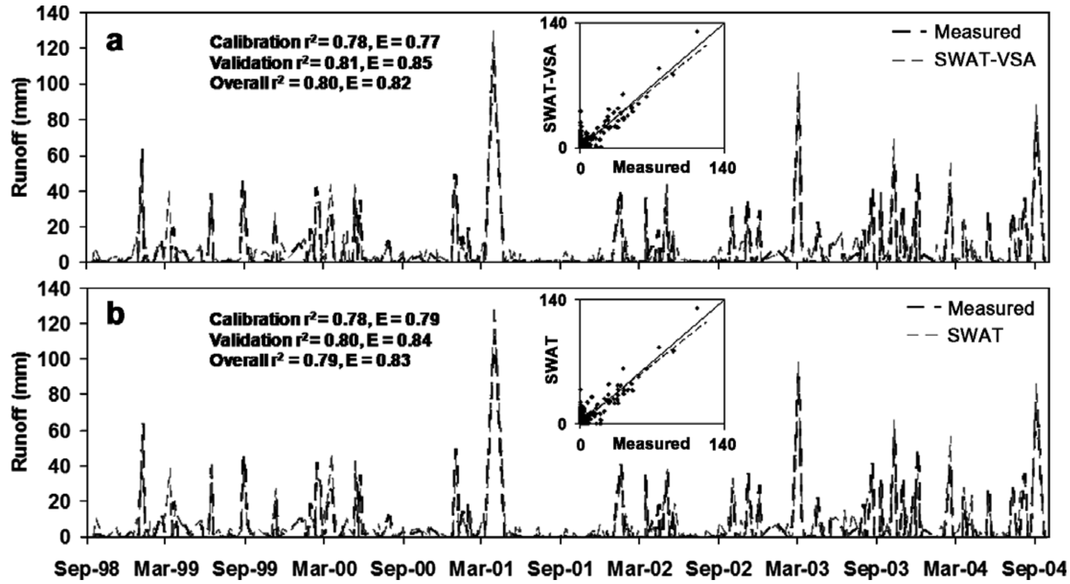

Figure 4 Event runoff predicted by SWAT-VSA (a) and SWAT (b) plotted against the measured baseflow separated runoff at the outlet of the watershed. Inset graphs show the linear 1:1 relationship.

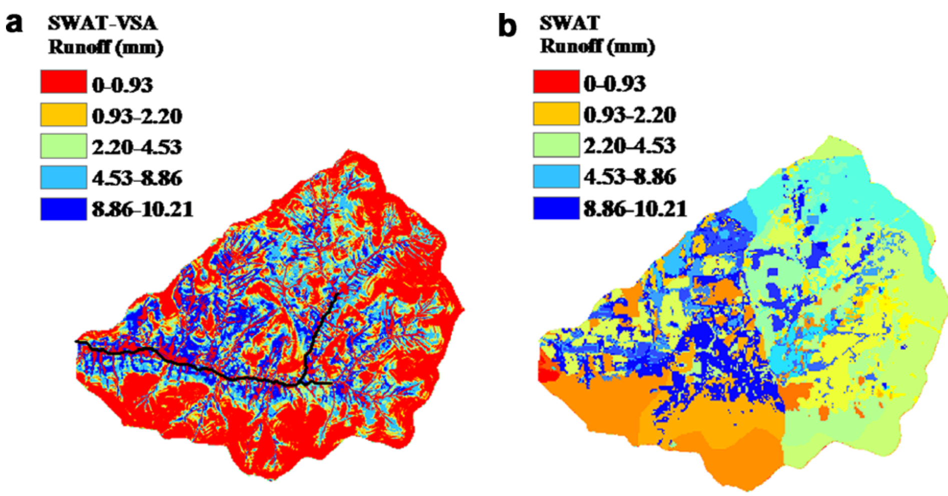

Figure 5 SWAT-VSA (a) and SWAT (b) predicted runoff distribution for an event in November 2003.

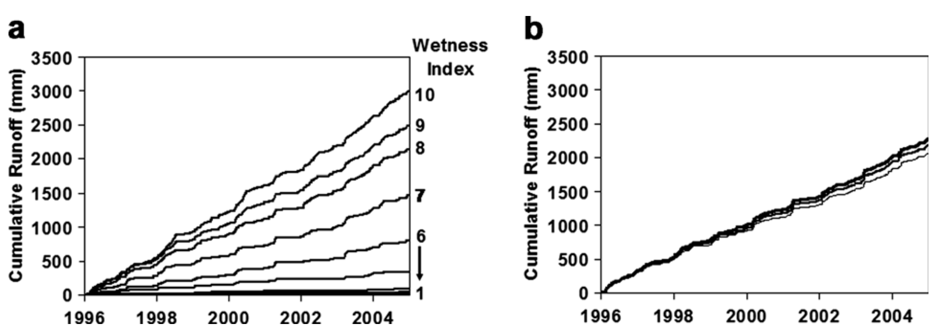

Figure 6 Cumulative runoff for watershed pastures for SWAT-VSA (a) and SWAT (b). Lines in subfigure b represent the cumulative runoff for pastures in each of the three sub-basins.

with pasture land uses, reflecting the three sub-basins in the model initialization. Intuitively, the runoff from pasture land use should not vary much among sub-basins, owing to the identical CN_{II} values. Slight variations are introduced due to different slopes and slope lengths in the sub-basins (Fig. 6b).

Water table depth

SWAT-VSA predicted soil water table height (above the restricting layer as indicated in the SSURGO database) agreed with measurements across the monitored hillside in the watershed with a $R^2 = 0.79$ (Fig. 7a). There was a slight tendency for SWAT-VSA to under predict water table height for large water table heights (Fig. 7a). SWAT, however, systematically under predicted water table height for all conditions (Fig. 7b). It should be noted that calibration of the *AWC* in SWAT could produce more accurate water table height predictions. However, this contradicts the idea that the model can be parameterized directly from the soils database, and would require extensive calibration that should, in general, be avoided. Under prediction by both models are probably somewhat due to the restricting layer depth being over estimated in the SSURGO data. Ground penetrating radar and geophone studies at the site (unpublished data, collected 2006–2007) show that the restricting layer is as close to the surface as 80 cm in some areas. Additionally, SSURGO porosity may be overestimated for this hillslope, which would consequently decrease predicted soil water table height. Indeed, the SSURGO reported porosity for the watershed soils was 50% for nearly all soils, while samples showed lower and more variable porosity (35–48%) (unpublished data, collected 2006).

Within a wetness index class, SWAT-VSA predictions mimicked the observed data, but tended to be less variable. Although this is noticeable in Fig. 7a, it becomes more apparent when data are plotted as a time series (data not shown). The lower variation in the SWAT-VSA predictions may be a consequence of a lack of lateral routing among HRUs or, conversely, the small time-scale variations in observed water table height may be partially due to the accumulation of upslope water and drainage to down slope areas. Even so, the longer-term variations appear to be well predicted by SWAT-VSA (Fig. 7a). In comparison, SWAT is not able to predict the water table height as accurately (Fig. 7b). For both the mixed forest and pasture the water table height is significantly underestimated.

The soil moisture content distribution in the watershed for SWAT-VSA and SWAT are shown in Fig. 8a and b. In accordance with VSA theory (Hewlett and Hibbert, 1967; Dunne and Black, 1970; Western et al., 1999; Beven, 2001; Niedzialek and Ogden, 2004; Western et al., 2004) a comparison of Figs. 5a and 8a show a direct relationship between runoff potential (Fig. 5a) and moisture contents (Fig. 8a). SWAT's runoff and soil water predictions (Figs. 5b and 8b, respectively) are not well correlated. For example, for the extreme west end of the watershed SWAT predicted its lowest runoff (the red area in Fig. 5b) and its highest soil water (blue in Fig. 8b). For SWAT-VSA areas of increased runoff necessarily have higher soil moisture levels as dictated by the saturation excess runoff theory in VSA hydrology.

Stream phosphorus

SWAT-VSA simulated event dissolved *P* fluxes substantially better than SWAT, $E > 0.75$ vs. $E < 0.5$, respectively (Fig. 9a and b). Furthermore, there was no obvious bias in SWAT-VSA predictions (inset Fig. 9a), whereas SWAT appeared to have a bias towards over-predicting dissolved *P* in the stream (inset Fig. 9b). Cumulative *P* loss from the basin was overestimated by 34% using SWAT vs. 10% with SWAT-VSA.

Recall that identical *P* application rates were used in SWAT-VSA and SWAT, and pasture and row crop generally have the most *P* available for transport because of manure and fertilizer applications. However, runoff patterns are variable within these land uses and, thus, some areas of pasture and row crop will contribute more and some areas less to the *P* load. SWAT-VSA was able to capture this variability and, presumably, this is why it predicted stream *P* loads, particularly peaks, more accurately than SWAT. For SWAT-VSA it is apparent that a relatively small portion of the watershed is responsible for the majority of the *P* loss while much of the area contributes little *P* (Fig. 10a). The underlying spatial patterns of dissolved *P* loss for SWAT-VSA (Fig. 10a) correspond to both the distribution of runoff predictions (Fig. 5a) and the areas of high *P* applications (i.e. manured or fertilized fields). Conversely, SWAT predicts most of the *P* loss originating from pasture or row crop essentially equally across the watershed (Fig. 10b). This,

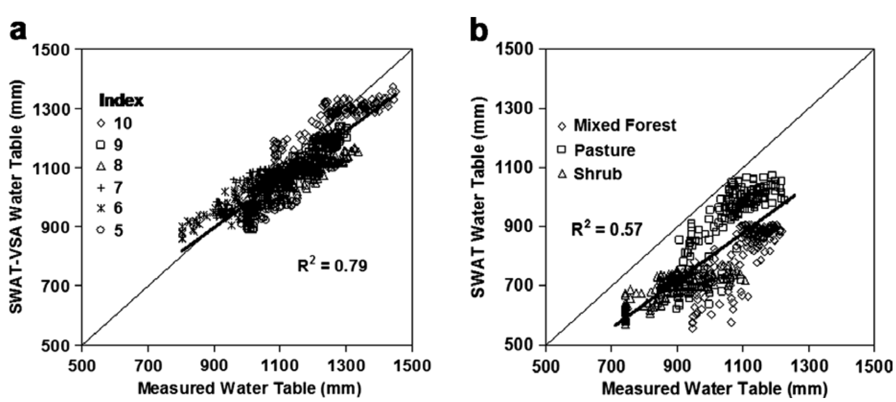

Figure 7 Relationship between SWAT-VSA (a) SWAT (b) predicted water table heights above the restricting layer by index class (SWAT-VSA) or land use (SWAT) and the measured water table heights for March 2004–September 2004 from Lyon et al. (2006a). Individual measured points within an index class or land use represent the average of the measurement within the respective classes for a single day.

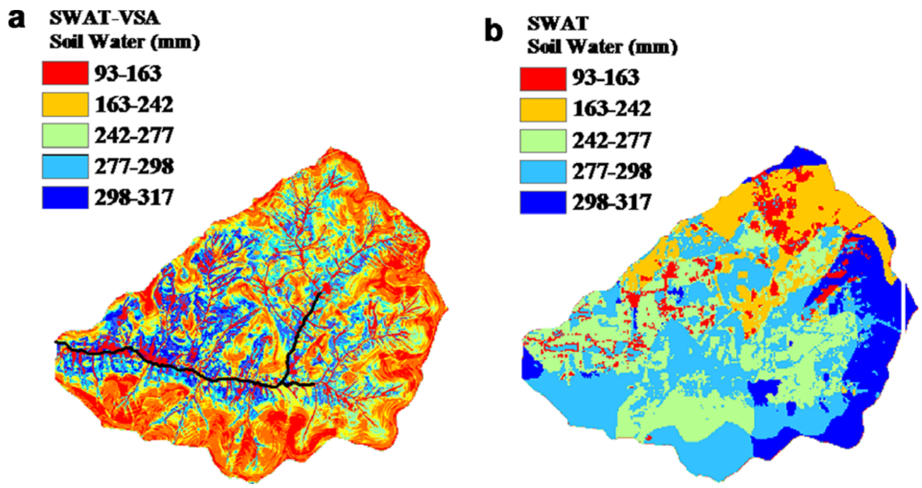

Figure 8 SWAT-VSA (a) and SWAT (b) predicted soil water distribution for an event in November 2003.

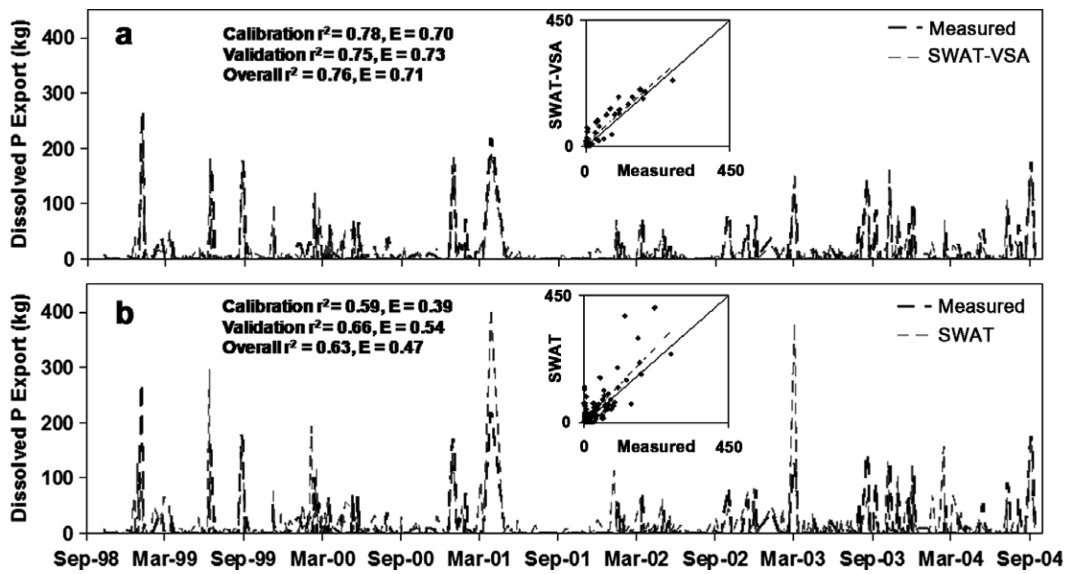

Figure 9 Event stream dissolved phosphorus export predicted by SWAT-VSA (a) and SWAT (b) plotted against the measured event stream dissolved phosphorus load. Inset graphs show the 1:1 relationship.

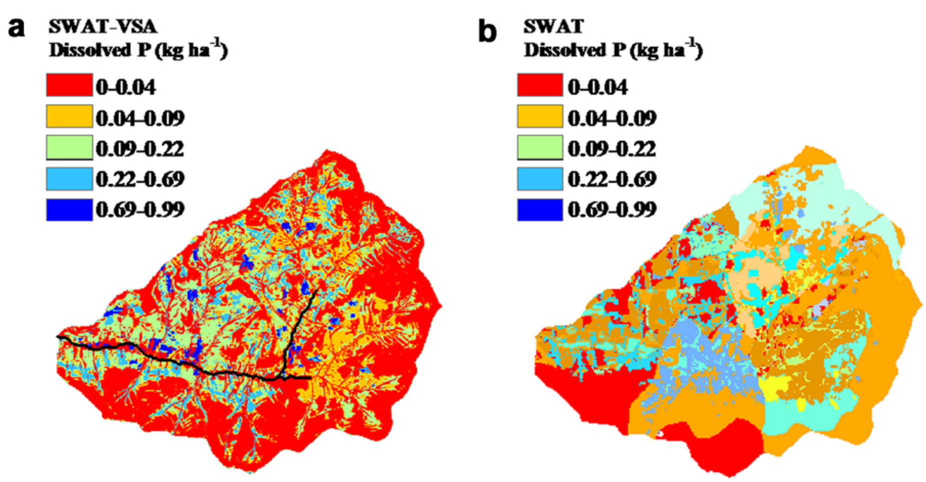

Figure 10 SWAT-VSA (a) and SWAT (b) predicted dissolved phosphorus (P) runoff loss distribution for an event in November 2003.

of course, follows from the fact that the original SWAT uses CN_{II} values that correlate runoff response to land use and soil type, and thus the only variation in *P* loss would be introduced by management practices.

An issue disputed between watershed modelers and field researchers is that nutrient loads predicted at small scales by models such as SWAT commonly underestimate the loss measured at the small scales (plot) and yet, in many cases, predictions match measured losses at the basin scale (Dr. Ray Bryant, USDA-ARS personal comm.). Indeed, several researchers have noted scale dependent effects when comparing results of lumped models with results measured at the plot scale (Amore et al., 2004; Miehle et al., 2006; Srivastava et al., 1998). Our results perhaps provide some anecdotal explanation of the phenomena. As noted earlier, in many regions runoff production is concentrated in relatively small fraction of a watershed, i.e., VSAs, and it is from these areas where concentrated pollutant losses are occurring. CN models like SWAT distribute the same volume of runoff over a much larger area and, thus, if they correctly predict the watershed scale *P* loss, they must generally underestimate losses from contributing areas and overestimate from non-contributing areas (Lyon et al., 2006b). Because SWAT-VSA appears to be more realistically capturing runoff producing areas, i.e., runoff is lost from small parts of the landscape, its predicted small-scale loads are likely in better agreement with those observed in plot-scale studies.

Implications

Accurate prediction of the spatial extent of runoff producing areas has consequences for simulation of pollutants that are transported by runoff. Many water quality protection strategies have been developed based on results from models like SWAT, which link runoff and pollutant concentrations almost solely to land use. As a result, we have sometimes dogmatically developed nonpoint source pollution control practices based too much on specific land uses and largely ignored the interaction between land management and physical, landscape scale processes like those that drive VSA hydrology. Garen and Moore (2005) explicitly noted this problem for current models that use the CN method. For example, our SWAT simulations suggest that landscape management of pollutants should be focused entirely on pastures and row crop (Fig. 10b). However, SWAT-VSA indicates that control of nutrients from areas near streams might be more logical locations to focus water quality protection efforts (Fig. 10a). Indeed, these results may help explain why riparian buffers are so effective, i.e., they keep potentially polluting activities out of areas most likely to generate runoff (Dosskey et al., 2002: Walter et al., 2005).

Summary and conclusions

Although the CN method is commonly used in ways that imply infiltration-excess runoff, previous work has shown that the method can be used in ways that describe saturation excess runoff processes from VSAs. In reality, the CN-equation is not based on any particular runoff generation mechanism. Mockus notes that S_e is either ''controlled by the rate of infiltration at the soil surface or by the rate of transmission in the soil profile or by the water-storage capacity of the profile, whichever is the limiting factor'' (Rallison, 1980). Interestingly, in later years he reportedly said ''saturation overland flow was the most likely runoff mechanism to be simulated by the method...'' (Ponce, 1996). We used this information to re-parameterize SWAT to account for runoff from VSAs, a re-conceptualization we call SWAT-VSA. We found that SWAT-VSA predicted distributed soil water and dissolved *P* loads leaving the watershed better than the original SWAT.

Ultimately, this re-conceptualization of SWAT provides a valuable tool for water resource planners and managers in regions with runoff from VSAs. For instance, many farms in the NYC water supply system in the Catskill Mountains are implementing BMPs to improve water quality, and models are currently being used to assess the current and future impact of the practices (Schneiderman et al., 2002, in press). In accordance with Schneiderman et al. (in press), we have shown that considering saturation excess runoff from VSAs provides a more realistic picture of the effectiveness of BMPs and, ultimately, produces more valid results. Thus, SWAT-VSA gives water resource managers another tool with which to assess and ultimately improve water quality practices.

Acknowledgements

This work was substantially supported by the Town Brook Research Group and we would like to note insights from Bil Gbuerk (USDA-ARS, retired), Michael McHale (USGS), Mark Zion (NYC-DEP), and Tamie Veith (USDA-ARS).

References

Agnew, L.J., Lyon, S., Gérard-Marchant, P., Collins, V.B., Lembo, A.J., Steenhuis, T.S., Walter, M.T., 2006. Identifying hydrologically sensitive areas: bridging science and application. J. Envir. Mgt. 78, 64–76.

Amore, E., Modica, C., Nearing, M.A., Santoro, V.C., 2004. Scale effect in USLE and WEPP application for soil erosion computation from three Sicilian basins. J. Hydrol. 293, 100–114.

Arnold, J.G., Allen, P.M., 1999. Automated methods for estimating baseflow and ground water recharge from streamflow records. J. Am. Water Resour. Assoc. 35, 411–424.

Arnold, J.G., Srinivasan, R., Muttiah, R.R., Williams, J.R., 1998. Large area hydrologic modeling and assessment part I: model development. J. Am. Water Resour. Assoc. 34 (1), 73–89.

Beven, K., 2001. Rainfall-Runoff Modeling: The Primer. John Wiley & Sons LTD, Chichester, England, p. 360.

Beven, K.J., Kirkby, M.J., 1979. A physically-based, variable contributing area model of basin hydrology. Hydrol. Sci. Bull. 24, 43–69.

Bhaduri, B., Harbor, J., Engel, B., Grove, M., 2000. Assessing watershed-scale, long-term hydrologic impacts of land-use change using a GIS-NPS model. Environ. Manag. 26, 643–658.

Borah, D.K., Bera, M., 2004. Watershed-scale hydrologic and nonpoint-source pollution models: review of applications. Trans. ASAE 47, 789–803.

de Alwis, D.A. 2007. Identification of hydrologically active areas in the landscape using satellite imagery. PhD Dissertation. Cornell University. Ithaca, NY.

Di Luzio, M., Srinivasan, R., Arnold, J.G., Neitsch, S.L. 2002. Soil and Water Assessment Tool. ArcView GIS Interface Manual: Version 2000. GSWRL Report 02-03, BRC Report 02-07, Published by Texas Water Resources Institute TR-193, College Station, TX. p. 346.

Dosskey, M.G., Helmers, M.J., Eisenhauer, D.E., Franti, T.G., Hoagland, K.D., 2002. Assessment of concentrated flow through riparian buffers. J. Soil Water Conserv. 57, 336–343.

Dunne, T., Black, R.D., 1970. Partial area contributions to storm runoff in a small New England watershed. Water Resour. Res. 6, 1296–1311.

Dunne, T., Leopold, L., 1978. Water in Environmental Planning. W.H. Freeman & Co., New York, p. 818.

Franchini, M., Pacciani, C., 1991. Comparative analysis of several rainfall runoff models. J. Hydrol. 122, 161–219.

Frankenberger, J.R., Brooks, E.S., Walter, M.T., Walter, M.F., Steenhuis, T.S., 1999. A GIS-based variable source area model. Hydrol. Proc. 13 (6), 804–822.

Garen, D.C., Moore, D.S., 2005. Curve number hydrology in water quality modeling: uses, abuses, and future directions. J. Am. Water Resour. Assoc. 41 (2), 377–388.

Haith, D.A., Shoemaker, L.L., 1987. Generalized Watershed Loading Functions for stream flow nutrients. Water Resour. Bull. 23 (3), 471–478.

Hewlett, J.D., Hibbert, A.R., 1967. Factors affecting the response of small watersheds to precipitation in humid regions. In: Sopper, W.E., Lull, H.W. (Eds.), Forest Hydrology. Pergamon Press, Oxford, pp. 275–290.

Horton, R.E., 1933. The role of infiltration in the hydrological cycle. Trans. AGU 14, 446–460.

Johnson, M.S., Coon, W.F., Mehta, V.K., Steenhuis, T.S., Brooks, E.S., Boll, J., 2003. Application of two hydrologic models with different runoff mechanisms to a hillslope dominated watershed in the northeastern US: a comparison of HSPF and SMR. J. Hydrol. 284, 57–76.

Krysanova, V., Muller-Wohlfeil, D.I., Becker, A., 1998. Development and test of a spatially distributed hydrological water quality model for mesoscale watersheds. Ecol. Model. 106, 261–289.

Lyon, S.W., Walter, M.T., Gerard-Marchant, P., Steenhuis, T.S., 2004. Using a topographic index to distribute variable source area runoff predicted with the SCS curve-number equation. Hydrol. Proc. 18, 2757–2771.

Lyon, S., Seibert, J., Lembo, A.J., Walter, M.T., Steenhuis, T.S., 2006a. Geostatistical investigation into the temporal evolution of spatial structure in a shallow water table. Hydrol. Earth Syst. Sci. Disc. 10, 113–125.

Lyon, S.W., McHale, M.R., Walter, M.T., Steenhuis, T.S., 2006b. The impact of runoff generation mechanisms on the location of critical source areas. J. Am. Water Resour. Assoc. 42, 793–804.

Mehta, V.K., Walter, M.T., Brooks, E.S., Steenhuis, T.S., Walter, M.F., Johnson, M., Boll, J., Thongs, D., 2004. Evaluation and application of SMR for watershed modeling in the Catskill Mountains of New York State. Environ. Model. Assess. 9 (2), 77–89.

Miehle, P., Livesley, S.J., Li, C.S., Feikema, P.M., Adams, M.A., Arndt, S.K., 2006. Quantifying uncertainty from large-scale model predictions of forest carbon dynamics. Global Change Biol. 12, 1421–1434.

Nash, J.E., Sutcliffe, J.V., 1970. River flow forecasting through conceptual models. Part I a discussion of principles. J. Hydrol. 10, 282–290.

Needelman, B.A., Gburek, W.J., Petersen, G.W., Sharpley, A.N., Kleinman, P.J.A., 2004. Surface runoff along two agricultural hillslopes with contrasting soils. Soil Sci. Soc. Am. J. 68, 914–923.

Niedzialek, J.M., Ogden, F.L., 2004. Numerical investigation of saturated source area behavior at the small catchment scale. Advan. Water Resour. 27 (9), 925–936.

NYCDEP (New York City Department of Environmental Protection), 2004. Multi tiered tater quality modeling program semi-annual status report- EPA filtration avoidance deliverable report. Valhalla, NY. July 2004.

Page, T., Haygarth, P.M., Beven, K.J., Joynes, A., Butler, T., Keeler, C., Freer, J., Owens, P.N., Wood, G.A., 2005. Spatial variability of soil phosphorus in relation to the topographic index and critical source areas: Sampling for assessing risk to water quality. J. Environ. Qual. 34, 2263–2277.

Ponce, V.M., 1996. Notes of my conversation with Vic Mockus. http://mockus.sdsu.edu.

Qui, Z., Walter, M.T., Hall, C., 2007. Managing variable source pollution in agricultural watersheds. J. Soil Water Conserv. 63 (3), 115–122.

Rallison, R.E., 1980. Origin and evolution of the SCS runoff equation. Symposium on Watershed Management. ASCE. New York, NY. pp. 912–924.

Ramanarayanan, T., Narasimhan, B., Srinivasan, R., 2005. Characterization of fate and transport of isoxaflutole, a soil-applied corn herbicide, in surface water using a watershed model. J. Agric. Food Chem. 53, 8848–8858.

Santhi, C., Arnold, J.G., Williams, J.R., Hauck, L.M., Dugas, W.A., 2001. Application of a watershed model to evaluate management effects on point and nonpoint source pollution. Trans. ASAE 44, 1559–1570.

Schneiderman, E.M., Pierson, D.C., Lounsbury, D.G., Zion, M.S., 2002. Modeling the hydrochemistry of the Cannonsville Watershed with generalized watershed loading functions (GWLF). J. Am. Water Resour. Assoc. 38 (5), 1323–1347.

Schneiderman, E.M., Steenhuis, T.S., Thongs, D.J., Easton, Z.M., Zion, M.S., Mendoza, G.F., Walter, M.T., Neal, A.L., in press. Incorporating variable source area hydrology into the curve number based generalized watershed loading function model. Hydrol. Proc. Available from: <http://www3.interscience.wiley.com/cgi-bin/fulltext/114295425/PDFSTART>.

Sharma, S.K., Mohanty, B.P., Zhu, J.T., 2006. Including topography and vegetation attributes for developing pedotransfer functions. Soil Sci. Soc. Am. J. 70, 1430–1440.

Srinivasan, M.S., Gburek, W.J., Hamlett, J.M., 2002. Dynamics of stormflow generation – a field study in east-central Pennsylvania, USA. Hydrol. Proc. 16 (3), 649–665.

Srinivasan, M.S., Gerard-Marchant, P., Veith, T.L., Gburek, W.J., Steenhuis, T.S., 2005. Watershed scale modeling of critical source areas of runoff generation and phosphorus transport. J. Am. Water Resour. Assoc. 41, 361–375.

Srivastava, P., Costello, T.A., Edwards, D.R., Ferguson, J.A., 1998. Validating a vegetative filter strip performance model. Trans. ASAE 41, 89–95.

Steenhuis, T.S., Winchell, M., Rossing, J., Zollweg, J.A., Walter, M.F., 1995. SCS runoff equation revisited for variable-source runoff areas. J. Irrig Drain. Eng. 121, 234–238.

Thompson, J.A., Pena-Yewtukhiw, E.M., Grove, J.H., 2006. Soil-landscape modeling across a physiographic region: topographic patterns and model transportability. Geoderma 133, 57–70.

US Army CERL, 1997, GRASS 5.3 users manual, Construction and Engineering Laboratory, Champaign IL.

USDA-NRCS, 2000. Soil Survey Geographic (SSURGO) database for Delaware County, New York, http://www.nrcs.usda.gov/products/datasets/sssurgo/.

USDA-SCS (Soil Conservation Service), 1972. National Engineering Handbook, Part 630 Hydrology, Section 4, Chapter 10.

van Griensven, A., Bauwens, W., 2003. Concepts for river water quality processes for an integrated river basin modeling. Water Sci. Tech. 48, 1–8.

Walter, M.T., Shaw, S.B., 2005. Discussion: ''Curve number hydrology in water quality modeling: uses, abuses, and future directions'' by Garen and Moore. J. Am. Water Resour. Assoc. 41 (6), 1491–1492.

Walter, M.T., Mehta, K., Marrone, A.M., Boll, J., Gérard-Merchant, P., Steenhuis, T.S., Walter, M.F., 2003. A simple estimation of the prevalence of Hortonian flow in New York City's watersheds. ASCE J. Hydrol. Eng. 8 (4), 214–218.

Walter, M.T., Gerard-Marchant, P., Steenhuis, T.S., Walter, M.F., 2005. Closure: a simple estimation of the prevalence of Hortonian flow in New York City's watersheds. ASCE J. Hydrol. Eng. 10 (2), 169–170.

Western, A.W., Grayson, R.B., Bloschl, G., Willgoose, G.R., McMahon, T.A., 1999. Observed spatial organization of soil moisture and its relation to terrain indices. Water Resour. Res. 35 (3), 797–810.

Western, A.W., Zhou, S.L., Grayson, R.B., McMahon, T.A., Bloschl, G., Wilson, D.J., 2004. Spatial correlation of soil moisture in small catchments and its relationship to dominant spatial hydrological processes. J. Hydrol. 286 (1–4), 113–134.

Williams, J.R., Jones, C.A., Dyke, P.T., 1984. The EPIC model and its applications. Proc. ICRISAT–IBSNAT–SYSS Symp. on Minimum Data Sets for Agrotechnology Transfer.